Characteristics of Fatigue Crack Initiation and Fatigue Strength of Nitrided 1Cr-1Mo-0.25V Turbine Rotor Steels

Chang-Min Suh*, Byung-Won Hwang
Department of Mechanical Engineering, Kyungpook National University, Taegu 702-701, Korea
Ri-Ichi Murakami
Department of Mechanical Engineering, Tokushima University, Tokushima 770-8506, Japan

To investigate the effect of nitriding layer on both fatigue crack initiation and fatigue life, turbine rotor steel (1Cr-1Mo-0.25V steel) specimens were nitrided by the nitemper method and then put to a rotary bending fatigue test at room and elevated temperatures. In nitriding, temperature and time were controlled to obtain a different nitrided thickness. Microstructure analysis, micro-Vickers hardness test, and scanning electron microscope observation were carried out for evaluating experiments. In results, the fatigue cracks of nitrided specimens were initiated at inclusion near the interface between nitrided layer and substrate, which showed fish-eye type appearance in fractograph. The fatigue life of nitrided specimens at every temperature was prolonged compared to that of the non-nitrided. However, there was not observable improvement in fatigue characteristics with the increase of a nitrided thickness.

Key Words : Nitriding, Fish-Eye Crack, Fatigue Strength, Fatigue Crack Initiation

1. Introduction

Machine components are required to work under more adverse conditions with the rapid development of technology ; for longer life, higher strength, and chemical stability of materials, studies on improving surface properties have become very important (Fuchs and Stephens, 1980).

Nitriding is a case hardening method that is used to improve the mechanical properties of metallic material. When compared with cementation that carbon is diffused into austenite, nitriding has an advantage in that the process is performed in a temperature range of 500~600℃ under the austenite transformation temperature. Accordingly, as there are only a little change in both substrate hardness and dimension during the process, nitriding has been used in the manufacture of die and precision parts for improving the resistance to wearing, corrosion, and fatigue load (Genel and Demirkol, 1999 ; 2000).

When compared with the established gas-nitriding method, soft-gas nitriding has certain advantages including a short nitriding time, applicability to all kinds of steel, and no by-product pollutants (Genel and Demirkol, 1999). In this study, the nitemper method, which is a form of soft-gas nitriding, was used for case hardening.

Nitriding also enhances the fatigue characteristics as it causes compressive residual stress reinforcing the surface layer (Yamamoto, et al., 1975 ; Kwak and Gil, 1985). In a rotary bending fatigue test, the fatigue limit of a nitrided specimen has been found to be higher than that of a non-nitrided specimen. Additionally, all cracks initiated on the surface are located close to the boundary between the nitride layer and the

* Corresponding Author,
E-mail : cmsuh@knu.ac.kr
TEL : +82-53-950-5573; **FAX** : +82-53-950-6550
Department of Mechanical Engineering, Kyungpook National University, Taegu 702-701, Korea. (Manuscript **Received** February 14, 2002; **Revised** May 27, 2002)

Table 1 Chemical compositions of 1Cr-1Mo-0.25V steel (wt, %)

C	Si	Mn	P	S	Cr	Mo	V	Ni	Al
0.29	0.24	0.76	0.0033	0.0006	1.10	1.19	0.24	0.46	0.0018

substrate (Yamamoto, et al., 1975; Qian and Fatemi, 1995).

However, previous studies were performed at room temperature without considering actual conditions. Therefore, in order to use nitirided steel as a rotating parts, like that turbine rotor or steam turbine blade, it is necessary to estimate the fatigue properties with taking actual working conditions into consideration. Accordingly, the purpose of this study was to investigate the effect of nitriding on the fatigue crack initiation and fatigue strength of turbine rotor steel (1Cr-1Mo-0.25V), at room temperature and elevated temperature (538℃) as well. Specimens were nitrided as different layer thickness by controlling the process time and temperature as parameters of the nitemper method. Thereafter, optical microscope observation, micro-Vickers hardness on the as-nitrided specimen, and SEM observation on the fatigue-fractured surface were carried out to analyze the effect of nitriding on fatigue characteristics.

2. Experimental Details

2.1 Specimens

2.1.1 Materials

A base material, tested in this study was 1Cr-1Mo-0.25V steel which is commonly used for a steam turbine rotor member. The chemical composition of this material is listed in Table 1. All the test specimens were machined from a forged cylindrical bulk material that was heated at 955℃, cooled with air blasting for 22 hours, and then reheated at 680℃ for 40 hours for a homogeneous microstructure.

2.1.2 Specimen preparation

Figure 1(a) shows a rotary bending fatigue test specimen with a diameter of 8mm and gage length of 8mm. Figure 1(b) shows the surface round

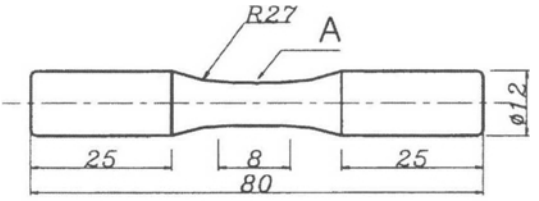

(a) Rotary bending fatigue specimen

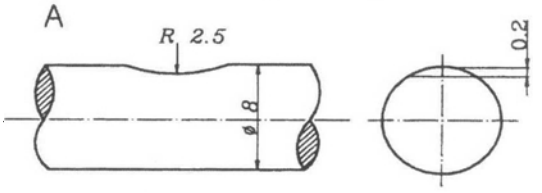

(b) Shallow transverse notch

Fig. 1 Configuration of specimen (unit : mm)

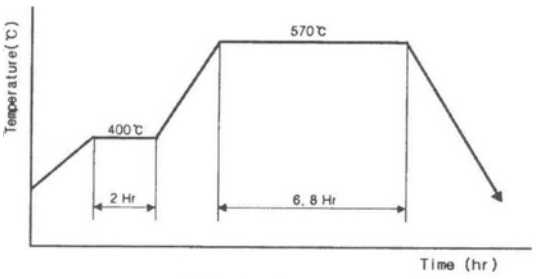

(a) Single stage

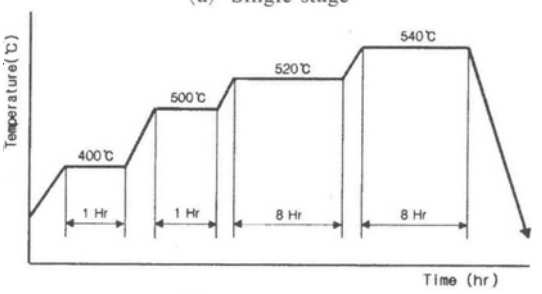

(b) Double stage

Fig. 2 Heat treatment cycles of nitriding

notch with a radius of 2.5mm and depth of 0.2mm, which was machined using a ball-type end mill in order to observe fatigue cracks without causing in the notch sensitivity.

Before nitriding, the gage length of the specimen was polished with emery papers up to #1500,

buffered with Cr_2O_3 powder, and cleaned in acetone solution.

2.1.3 Nitriding of specimens

The nitemper method was used in this study for nitriding. Two kinds of heat-treatment cycles, named single and double stage nitridings, were performed to change the thickness of compound layers, formed at the surface affecting on the fatigue characteristics. Figure 2 illustrates the heat-treatment cycles of the nitriding process used in this study. Nitriding time for the single stage treatment shown in Fig. 2(a) was set to 6 and 8 hours at 570℃ to make different nitrided layers. In the double stage shown in Fig. 2(b), nitriding time was set to 8 hours at 520℃ and 8 hours at 540℃.

2.2 Tests and Observation

2.2.1 Microstructure observation

The nitrided specimen was mirror-polished and etched with 5% Nital in order to observe the microstructure. Microstructures from the edge to the center of an etched specimen were observed by using a metallograph and photographs were taken by an attached camera.

2.2.2 Hardness test

In order to measure the hardness profile of nitrided layer, a micro-Vickers hardness tester (HMV-2000, Shimadzu) was used. An indentation load of 25g was applied for 30 seconds to measure the hardness of the nitride diffused range. However, only a 10g of indentation load was used to measure the compound layer because of a very thin thickness.

2.2.3 Rotary bending fatigue test

Fatigue tests were conducted using an Ono-type rotary bending fatigue tester to investigate the effect of nitriding on the fatigue crack initiation and the fatigue strengths of specimens at room temperature and 538℃. To elevate the temperature of a specimen to 538℃, an electric resistance furnace of 1/2 snatch of tubular separation type was used. Test temperature of specimen was measured by K-type thermocouple through the small hole in the center of the electric furnace, and controlled within 538±3℃ by using the automatic temperature controller.

2.2.4 Fractography analysis

The fatigue-fractured surfaces were observed by SEM. The applied stress, the crack initiation position and the area of fish-eye crack were then analyzed. In addition, X-ray energy dispersive spectroscopy (EDS) was used to clear the chemical composition of inclusion within fish-eye type crack.

3. Results and Discussion

3.1 Microstructure of nitrided layer

Figure 3 shows the microstructure of a nitrided region that was generated by the single stage in the nitriding process for 6 hr at 570℃. As seen in Fig. 3, the nitride layer is composed of the compound layer and the diffusion layer and the layer thickness were formed differently according to the nitriding methods. The thickness of the compound layers measured 6.9μm for double stage and 19.2μm and 14.0μm for 6 hr and 8 hr single stage, respectively.

3.2 Hardness variation and thickness of nitrided layer

The micro-Vickers hardness profiles from edge

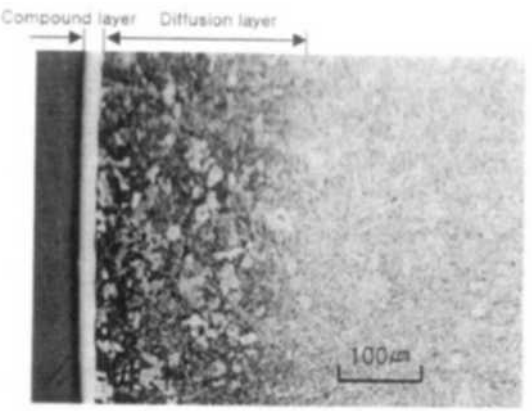

Fig. 3 Microstructure of nitrided layer formed by the single stage heating cycle for 6 hr at 570℃

Table 2 The depth of compound and diffusion layer

Temperature-Time	Depth of nitrided layer		
	Compound layer	Diffusion layer	Total layer
520℃-8hr 540℃-8hr	6.9μm	153.1μm	160μm
570℃-6hr	19.2μm	230.8μm	250μm
570℃-8hr	14.0μm	276.0μm	290μm

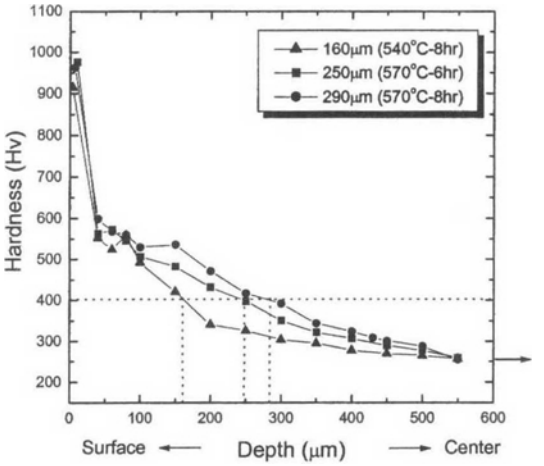

Fig. 4 Micro-Vickers hardness profiles and nitrided depth with different nitriding process

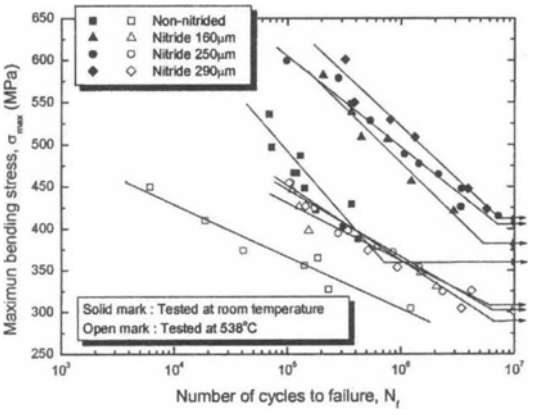

Fig. 5 Relationship between maximum bending stress, σ_{max} and number of cycles to failure, N_f at room temperature and 538 ℃

to center direction are shown in Fig. 4 with the different nitriding processes. The hardness values apart from the surface of the nitrided specimen (260 Hv) were similar to those of the non-nitrided specimen. The hardness values of the compound layer were about 950 Hv but rapidly decreased in the diffusion layer. They fell to 260 Hv at the 500 μm from the surface, which were similar to those of the non-nitrided specimen.

According to the references (Genel and Demirkol, 2000), the case depth, in this study, was defined as the position from the surface that had 400 Hv. By this criterion and from Fig. 4, the thickness of nitride layers were obtained as 160μm for double stage process and 250μm and 290μm for 6 hr and 8 hr single stage process, respectively.

Table 2 summarizes the depth of a total nitride layer, a compound layer, and a diffusion layer, which were produced by the different nitriding processes. In Table 2, the heat treatment temperature is more effective than the time on the nitriding depth. However, because the compound layer makes a detrimental effect on the material surface for fatigue characteristics, the thickness of a compound layer and a diffusion layer should be harmonized with the proper process parameters.

3.3 Fatigue life and strength

Figure 5 shows the S-N relationship between the maximum bending stress, σ_{max} and the fatigue life, Nf at room temperature and 538℃ for the 160μm, 250μm, and 290μm nitrided and non-nitrided specimens. The fatigue life of the nitrided specimens was improved greatly compared with that of the non-nitrided specimens under all the stress levels applied in this study. The fatigue limit of the nitrided specimens at room temperature also increased with the thickness of nitrided layer. Compared with the non-nitrided specimen, the fatigue life of the 290μm nitrided specimen was improved as 17 times at 500MPa and 28 times at 446MPa. In addition, the fatigue limits of

nitrided specimens were also improved by 7% for 160μm, 14% for 270μm, and 17% for 290μm.

Similar behaviors on the high temperature fatigue life and fatigue limit can be observed in Fig. 5. However there can be seen a little difference in fatigue properties with altering the layer thickness.

At all applied stress levels, it would appear that the improvement of the fatigue life by nitriding may be attributed to the retardation of crack initiation due to the restriction of the surface plastic deformation in the substrate as a result of a hard nitrided layer (Qian and Fatemi, 1995; Magnusson, 1973; Gustavsson and Melander, 1992).

In general, the fatigue life of steel is decreased with increase of test temperature. This is due to the degradation of mechanical properties and the local plastic deformation that is concentrated by an initiation of micro cracks in the oxide layer at elevated temperature (Suh and Kitagawa, 1987; Lankford, 1997). However, fatigue cracks in the nitrided specimens tested in this study were not initiated on the surface but in the inside. This is due to hardened surface layer and compressive residual stress of the nitriding process (Murakami, 1989; Murakami and Usuki, 1989). Thus the effects of the degeneration and the oxide layer of the surface are negligible.

3.4 Fatigue crack initiation and growth behaviors

Under the high cycle fatigue loadings, the fatigue crack of a smooth metal specimen initiates from the inclusion formed during cyclic loading and became a source of local stress concentration (Fuchs and Stephens, 1980). Therefore, by improving surface hardness, the initiation of a fatigue crack can be retarded by restraining the dislocation movement on the surface (Qian and Fatemi, 1995; Magnusson, 1973). If it is hard enough to prevent slip deformation on the specimen surface due to the relatively less applied stress, the fatigue crack should be made at other position. Therefore, it is possible that a fatigue crack may occur due to stress concentration at a void or an inclusion that exists at a position close to the specimen surface but not hardened (Genel and Demirkol, 1999; 2000).

Figure 6 shows a fractograph of the fish-eye (Fig. 6(a) and 6(c)) and the final fracture pattern (Fig. 6(b) and 6(d)) at room temperature and 538℃ for the 250μm nitrided specimen. As shown in figures, the typical fish-eye cracking which is usually found in high-strength steels (Suh, et al., 1999; Suh and Kitagawa, 1987; Murakami, 1989) was observed and all the

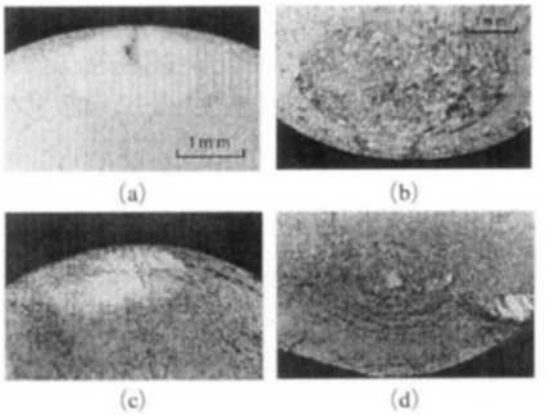

Fig. 6 Fractographs of fish-eye and final fracture pattern for 250μm nitrided specimen: (a) and (b) at σ_a=407MPa, N_f=1.05×107, RT; (c) and (d) at σ_a=454MPa, N_f=1.04×105, 538℃

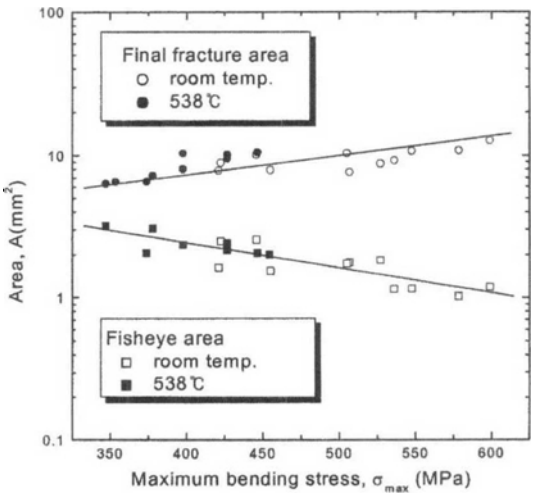

Fig. 7 Behaviors of the fish-eye and the final fractured area with the maximum applied bending stress

nitrided specimens fractured in the fatigue test showed fish-eye cracks.

The area of the fish-eye crack, which is white and look like an elliptical circle, and final fracture region were quantitatively measured to clarify the initiation and growth behavior of fatigue crack in the nitrided specimens. The area of the fish-eye crack and the final fracture measured by a metallograph were then analyzed with the maximum applied bending stress. Figure 7 shows the behavior of the areas of final fracture with the applied bending stresses. As seen in Fig. 7, the areas of fish-eye crack and final fracture changed linearly with applied stress in the semi-log plot for the specimens tested at room and elevated temperature.

3.5 Observation of fatigue-fractured surface

The fatigue-fractured surfaces were observed with SEM and the inclusion at the crack initiated sites was analyzed with X-ray energy dispersive spectroscopy (EDS) to clarify the crack initiation.

Figure 8 shows examples of low and high magnification SEM observation of the fish-eye formed in the 160μm nitrided specimen fractured under 536.1MPa at room temperature. In Fig. 8 (a), the square mark indicates the center of the fish-eye crack and the fatigue crack initiated and grew from this site. Figure 8(b) shows an inclusion at the center of square mark in Fig. 8(a). As inclusions in the steel become a cause for stress concentration, it is observed that the initial fatigue crack generated in this position and then propagated. In addition, the fish-eye crack of this specimen was due to the internal cracking that frequently occurred in high-strength steel (Murakami, 1989 ; Gabetta and Torri, 1992 ; Murakami, et al., 1989).

Figure 8(c) shows the result of the EDS analysis at the inclusion; its chemical components were Al and Ca that remained in the ingot for making killed steel. Al and Ca are used for deoxidation processes such as ABS method (Alloy Bullets Shooting method) and SCAT method (Shooting Calcium Adding Technique method). If Al and Ca were not completely removed, oxides of Al and Ca remained in the material as inclusions, which became a source of fatigue crack initiation (Suh, et al., 1999).

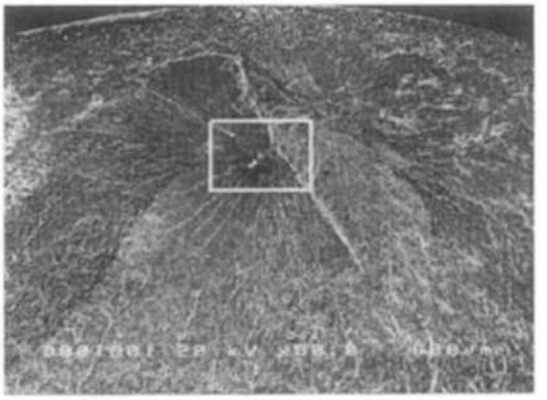

(a) Fish-eye crack (×50)

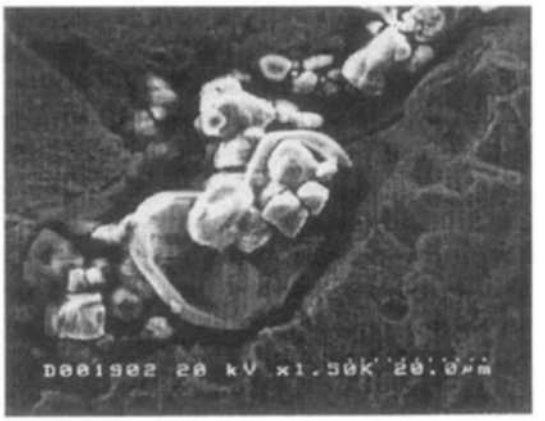

(b) Inclusion (×1500)

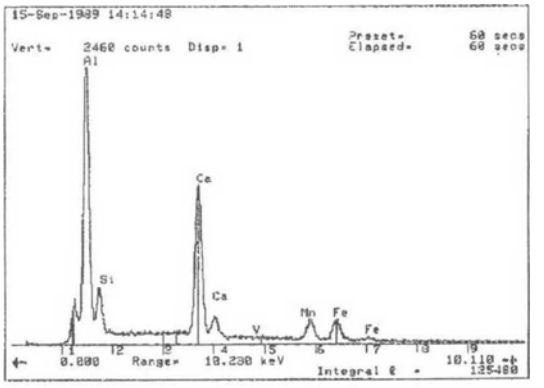

(c) EDS analysis

Fig. 8 SEM fractographs and EDS analysis at fish-eye crack (nitride thickness=160μm, σ_a=536.1MPa, N_f=3.56×105 cycles, RT)

3.6 Effect of inclusion on fatigue strength

Figure 9 shows the relationship between the maximum applied bending stress and the location of initial crack from the specimen surface. The initiation sites of fatigue cracks move toward the specimen surface as the applied bending stress increase at both room temperature and 538℃. In addition, all of the inclusion were found at a distance of over 500μm from the surface. As the positions were not hardened by nitriding, it was expected that the complex effects including the residual stress and the constraint of hardened layer have an effect on the crack initiation.

The fatigue limit of nitrided hardening relative to the variation of the interior defect size can be evaluated by using the formula proposed by Murakami (1989). Equation (1) and (2) are the evaluation formula proposed by Murakami for the fatigue limits (σ_ω) of the case hardened steels by nitriding without and with regard of residual stress, respectively.

$$\sigma_\omega=\frac{1.56(Hv+120)}{(\sqrt{area})^{1/6}} \tag{1}$$

$$\sigma_\omega=\frac{1.56(Hv+120)}{(\sqrt{area})^{1/6}}\cdot[(1-R)/2]^{\alpha} \tag{2}$$

where, Hv is the micro-Vickers hardness, R is the stress ratio defined as $[(\sigma_{res}-\sigma_a)/(\sigma_{res}+\sigma_a)]$, and α is $0.226+Hv\times10^{-4}$.

Figure 10 is the fatigue limit that is obtained in the S-N curve and Eq. (1) with the area of inclusion. The fatigue limits obtained at room temperature test showed 1.5 times higher values than the calculated ones. However, at the elevated temperature test, fatigue limits fell close to the calculated line. This is considered as the effect of the residual stress relaxation and the softening of material at high temperature. Compressive residual stress is calculated as 320MPa for 400MPa of alternating stress by using Eq. (2).

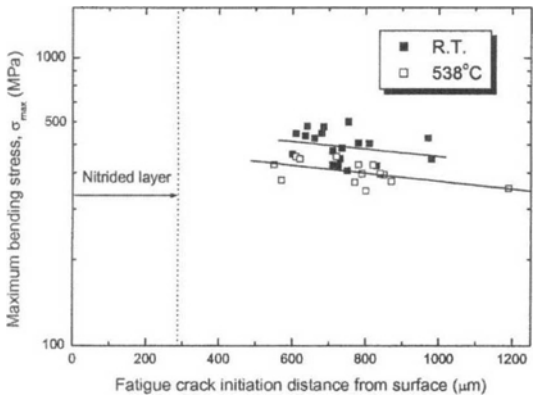

Fig. 9 Relationship between the maximum bending stress, σ_{max} and the distance from surface to crack initiated position

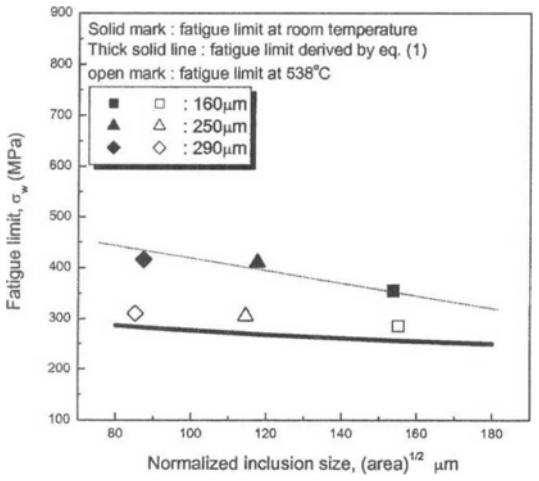

Fig. 10 Fatigue limits, σ_w with the variation of inclusion size ($\sqrt{area}$)

4. Conclusions

To investigate the effect of nitriding on fatigue crack initiation and fatigue strength, rotary bending fatigue tests were carried out in air atmosphere using nitrided 1Cr-1Mo-0.25V steel specimens at room temperature and 538℃. The following results were obtained:

(1) The surface hardness of the nitrided steel was improved by 3 times higher at the compound layer than the substrate. In addition, the fatigue life of nitrided specimens were highly improved at both room temperature and 538℃.

(2) The fatigue crack of the nitrided steel was initiated from an inclusion located in the substrate. This was due to the hardened layer that retarded the initiation of a fatigue crack by constraining the plastic deformation.

(3) A fish-eye crack was observed on the fractured surface and chemical compositions of

the inclusion, which initiated the fatigue crack, were Al and Ca.

(4) The size and location of the inclusion, the residual stress, and hardness were important factors on fatigue strength.

Acknowledgment

This work was supported by the Brain Korea 21 Project.

References

Fuchs, H. O. and Stephens, R. I., 1980, *Metal Fatigue in Engineering*, John Wiley & Sons, Pub., pp. 27~34.

Gabetta, G. and Torri, L., 1992, "Crack Nucleation and Propagation in Blade Steel Material," *Fatigue Fracture Engineering Materials Structure*, Vol. 15, No. 11, pp. 1101~1111.

Genel, K. and Demirkol, M., 1999, "Effect of Case Depth on Fatigue Performance of AISI 8620 Carburized Steel," *International Journal of Fatigue*, 21, pp. 207~212.

Genel, K., Demirkol, M. and Capa, M., 2000, "Effect of Ion Nitriding on Fatigue Behavior of AISI 4140 Steel," *Materials Science & Engineering*, A279, pp. 207~216.

Gustavsson, A. I. and Melander, A., 1992, "Fatigue Limit Model for Hardened Steels," *Fatigue Fracture Engineering Materials Structure*, Vol. 15, No. 9, pp. 881~894.

Kwak, B. M. and Gil, Y. J., 1985, "An Indirect Experimental Method for the Determination of Mechanical Properties of Ion-nitrided Layer and Residual Stress Distribution," *Transaction of the Korean Society of Mechanical Engineers*, Vol. 9, No. 2, pp. 240~249.

Lankford, J., 1997, "Initiation and Early Growth of Fatigue Cracks in High Strength Steel," *Engineering Fracture Mechanics*, Vol. 9, pp. 617~624.

Magnusson, L., 1973, "Low Cycle Behavior of Case Hardened Steel," Mechanisms of Deformation and Fracture, pp. 105~110.

Murakami, Y., 1989, "Effect of Small Defects and Nonmetallic Inclusions on the Fatigue Strength of Metals," *JSME International Journal*, Vol. 32, No. 2, pp. 167~180.

Murakami, Y. and Usuki, H., 1989, "Prediction of Fatigue Strength of High-Strength Steels Based on Statistical Evaluation of Inclusion Size," *Journal of JSME*, A55, No. 510, pp. 213~221.

Murakami, Y., Kodama, S. and Konuma, S., 1989, "Quantitative Evaluation of Effects of Non-metallic Inclusions on Fatigue Strength of High Strength Steel. I : Basic Fatigue Mechanism and Evaluation of Correlation between the Fatigue Fracture Stress and the Size and Location of Non-metallic Inclusions," *International Journal of Fatigue*, Vol. 11, No. 5, pp. 291~298.

Qian, J. and Fatemi, A., 1995, "Cyclic Deformation and Fatigue Behavior of Ion-Nitrided Steel," *International Journal of Fatigue*, Vol. 17, No. 1, pp. 15~24.

Suh, C. M. and Kitagawa, H., 1987, "Crack Growth Behavior of Fatigue Microcracks in Low Carbon Steels," *Fatigue Fracture Engineering Materials Structure*, Vol. 9, No. 6, pp. 409~424.

Suh, C. M., Kim, K. R. and Lee, D. W., 1999, "Fatigue Strength of TiAlN Ceramic Coated 1Cr-1Mo-0.25V Steel at Elevated Temperatures," *International Journal of Ocean Engineering and Technology*, Vol. 1, No. 1, pp. 69~76.

Yamamoto, K., et al., 1975, "The Comparison of Properties in Iron-nitrided and un-nitrided Specimen," *Japanese Metallic Material*, Vol. 15, No. 7, pp. 26~37.